2011 American Control Conference
on O'Farrell Street, San Francisco, CA, USA
June 29 - July 01, 2011

Optimal Control Architecture Selection for Thermal Control of Buildings

Vikas Chandan and Andrew G. Alleyne

***Abstract*— The problem of partitioning a building into clusters is considered in this paper, with reference to its decentralized thermal control. Optimal control schemes for these systems are often centralized and address both the thermal comfort and energy efficiency requirements. However, due to robustness considerations, a decentralized architecture may be preferred for large scale systems, which is at best sub-optimal. Therefore, the 'degree of decentralization' governs the trade-off between optimality and robustness. This paper proposes a combinatorial optimization based systematic methodology for obtaining an optimal degree of decentralization on the basis of two metrics - one for optimality (defined as Coupling Loss Factor) and one for robustness (defined as Mean Cluster Size). The methodology was evaluated on a building model and results were found to be in agreement with the physics of the underlying thermal interactions.**

I. INTRODUCTION

The building sector accounts for around 41% of the annual energy consumption and almost the same share of greenhouse gas emissions in the United States [1]. This has motivated the use of advanced control techniques, e.g. model predictive control (MPC) [2], [3] and hardware, e.g. BACnet [4] for the intelligent control of buildings. In particular, the control of the heating, ventilation and air-conditioning (HVAC) systems has received much attention [5], [6], because more than one-third energy usage in buildings can be attributed to zone heating and cooling.

For large scale systems, such as buildings, the performance of the control system is correlated with the choice of the control architecture. In theory, a centralized controller, with knowledge of a perfect model of the system and access to building-wide sensor data, could control the building optimally. A key limitation of centralized decision making, however, is its potentially inferior robustness to sensor and communication network failures.

Decentralized control is more resilient to such failures and also easier to design and tune [7]. However, a decentralized controller ignores any coupling between the particular subsystem that it controls and the rest of the plant. This may result in suboptimal performance. Therefore, it is imperative to choose a control architecture which lies between the two extremes of completely centralized control and fully decentralized control. In this regard, multi-agent distributed and decentralized control architectures, which provide limited or no communication among the controllers has been advocated for buildings [8], [9], [10], [11], [12], [13]. However, the underlying control architecture is chosen in a somewhat heuristic manner, on the basis of the building topology or functional separation of the building subsystems. In the present work, we propose a systematic methodology to determine the control clusters in a building for implementing a control architecture, which is decentralized with respect to the clusters. The choice of the appropriate clusters is based on the afore-mentioned trade-off between optimality and robustness as characterized by appropriate metrics, and involves combinatorial optimization. The proposed approach relies on an MPC framework, because MPC has been studied extensively for the control of building systems [2], [3], [14].

Alleyne (alleyne@illinois.edu) and Chandan are with the Department of Mechanical Science and Engineering, University of Illinois, Urbana, IL 61801, USA

The organization of this paper is as follows. Some preliminaries are discussed in Section II. Section III describes the proposed clustering procedure. A simulation case study is provided in Section IV where the clustering technique is implemented on a building model. Lastly, the conclusions are summarized in Section V.

II. PRELIMINARIES

A. Open Loop Model

A resistive-capacitive (RC) network is typically used to represent a lumped model of building thermal dynamics [15], [16], [17]. The ensuing linear state space model in discrete time is of the following form :

$$x(k+1) = Ax(k) + B_u u(k) + B_w w(k) \tag{1}$$

$$y(k) = Cx(k) \tag{2}$$

In this model, $x = \left({T_w}^T\ {T_z}^T\right)^T$ is the state vector consisting of the building wall and zone-air temperatures. The vectors u and w represent control inputs and disturbances respectively. The control inputs consist of energy transfer rates (positive for heating) between the air-conditioning system and the zones. The unmodeled thermal loads in the zones and the ambient air temperature are treated as disturbances. The outputs are the zone-air temperatures, i.e. $y = T_z$, which can be measured using thermostats. The number of control inputs and controlled outputs are denoted by N_u and N_y respectively. In this work, both these quantities equal the number of rooms in the building.

B. MPC Framework

The objective function for optimal building thermal control is usually a weighted sum of objectives representing thermal comfort and air conditioning power consumption [5]. With reference to the model described above, we use the following objective function [1] to be minimized at each time instant k, for a discrete-time MPC implementation :

$$J_k = \underbrace{\sum_{j=0}^{N-1} \alpha^T u\left(k+j|k\right)}_{\textit{Power consumption term}} + \underbrace{\alpha_2 \sum_{j=1}^{N} \left|\left|y\left(k+j|k\right) - y_{ref}\left(k\right)\right|\right|_2^2}_{\textit{Thermal comfort term}} \quad (3)$$

Here N is the number of samples in the prediction and control horizon; $\{y\left(k+j|k\right)\}_{j=1}^{N}$ is the predicted output sequence over the prediction horizon, based on the model ((1) and (2)), when the control sequence $\{u\left(k+j|k\right)\}_{j=0}^{N-1}$ is applied; $y_{ref}\left(k\right)$ is the desired (reference) value of the output at the current time instant, k. The purpose of the optimization is to find the optimal control sequence $\{u^*\left(k+j|k\right)\}_{j=0}^{N-1}$ that minimizes J_k.

C. Coupling between inputs and clusters of inputs

J_k can be expresssed as a quadratic function of the control sequence $\{u\left(k+j|k\right)\}_{j=0}^{N-1}$, by successive substitution of (1) and (2) in (3) [18].

$$J_k = {v_k}^T H_k v_k + {f_k}^T v_k \quad (4)$$

Where :

$$v_k = \left(\bar{u}_1^T \bar{u}_2^T .... \, \bar{u}_{N_u}^T\right)^T,$$
$$\bar{u}_i = \left(u_i\left(k|k\right) u_i\left(k+1|k\right) .... \, u_i\left(k+N-1|k\right)\right)^T,$$
$$i = 1, 2, ... \, N_u$$

Here, u_i denotes the i^{th} component of u. The quadratic part, ${v_k}^T H_k v_k$, can be written in the expanded form as :

$$\begin{pmatrix} \bar{u}_1 \\ \bar{u}_2 \\ . \\ . \\ . \\ \bar{u}_{N_u} \end{pmatrix}^T \begin{pmatrix} H_{1,1} & H_{1,2} & .. & H_{1,N_u} \\ H_{2,1} & H_{2,2} & .. & H_{2,N_u} \\ . & . & .. & . \\ . & . & .. & . \\ . & . & .. & . \\ H_{N_u,1} & H_{N_u,2} & .. & H_{N_u,N_u} \end{pmatrix} \begin{pmatrix} \bar{u}_1 \\ \bar{u}_2 \\ . \\ . \\ . \\ \bar{u}_{N_u} \end{pmatrix}$$

Each off-diagonal term, $H_{i,j} \in \mathbb{R}^{N \times N}, i \neq j$ represents the coupling between u_i and u_j in J_k. Therefore, we use $\left|\left|H_{i,j}\right|\right|_2$ as a measure of coupling [2] between u_i and u_j and extend this to define coupling between between a pairs of input clusters.

Consider a pair of input clusters, C_1 and C_2. The coupling matrix between these clusters, H_{C_1,C_2} is defined as :

$$H_{C_1,C_2} = \begin{pmatrix} H_{p_1,q_1} & H_{p_1,q_2} & ... \\ H_{p_2,q_1} & H_{p_2,q_2} & ... \\ . & . & ... \\ . & . & ... \\ . & . & ... \end{pmatrix} \quad (5)$$

Where,

$$p_1, p_2 \,...\in C_1 \text{ and } q_1, q_2 \,...\in C_2$$

The coupling $\boldsymbol{\mathcal{C}}\left(C_1, C_2\right)$, between C_1 and C_2, is then defined as :

$$\boldsymbol{\mathcal{C}}\left(C_1, C_2\right) = \left|\left|H_{C_1,C_2}\right|\right|_2 \quad (6)$$

III. CLUSTERING PROCEDURE

The clustering procedure is carried out in a divisive sequence as illustrated in Fig. 1. The input to each stage is a set of *parent clusters*, and the output is a set of *child clusters*. The child clusters are obtained from the parent clusters via combinatorial analysis. The input to the first stage is the root cluster containing all the control inputs, which represents the completely centralized case. The output of the last stage is a set where each control input is a cluster by itself and hence represents a fully decentralized architecture. For any intermediate stage S_i, the input (set of parent clusters) is the same as the output (set of child clusters) of the previous stage S_{i-1}. Two metrics representing optimality and robustness are computed for each stage. A plot of one metric versus the other is then used to identify the stage which results in a satisfactory tradeoff between robustness and optimality.

A. Optimality and robustness metrics

Two dimensionless metrics - Coupling Loss Factor (CLF) and Mean Cluster Size (MCS) are computed for each partitioning stage.

1) CLF: The CLF for stage S_i is a normalized measure of the inter-cluster coupling among its child clusters that are denoted by C_i^j, where $j = 1, 2, ..., n_i$. Here, n_i is the total number of such child clusters. First, we introduce the coupling loss vector μ_i for this stage S_i as the vector of the couplings $\boldsymbol{\mathcal{C}}\left(C_i^p, C_i^q\right)$ for each pair of child clusters, C_i^p and C_i^q, with $p \neq q$. More formally :

$$\mu_i = \left(\mu_{i,1} \quad \mu_{i,2} \quad ... \quad \mu_{i,n_i}\right)^T \quad (7)$$

where,

$$\mu_{i,p} = \left(\boldsymbol{\mathcal{C}}\left(C_i^p, C_i^{p+1}\right) \quad \boldsymbol{\mathcal{C}}\left(C_i^p, C_i^{p+2}\right) \quad ... \quad \boldsymbol{\mathcal{C}}\left(C_i^p, C_i^{n_i}\right)\right),$$
$$p = 1, 2, ...n_i$$

1. It is assumed that all rooms of the building are simultaneously under heating or cooling. This allows the representation of the power consumption term using a linear function of the control inputs.

2. It is important to scale the system first so that coupling values corresponding to different pairs of input channels can be compared with one another. For a discussion on scaling see [19].

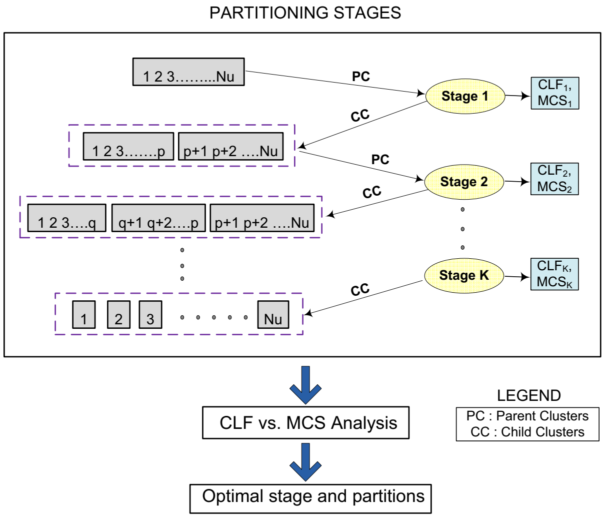

Fig. 1. Overview of clustering procedure.

The CLF for stage S_i, CLF_i is then defined as :

$$\text{CLF}_i = \frac{||\mu_i||_2}{||H_k||_2} \tag{8}$$

The CLF for the parent cluster to stage 1, which represents the fully centralized scenario, is clearly zero. CLF_i measures the coupling that is ignored if the system were partitioned according to the child clusters of stage S_i. Therefore, it is desired to partition the system such that the corresponding CLF is small, thus resulting in small deviation in optimality from centralized control.

2) MCS: We use λ_i^j to denote the number of elements in child cluster C_i^j. MCS_i for stage S_i is the average number of elements per child cluster normalized with respect to the total number of control inputs.

$$\text{MCS}_i = \frac{\sum_{j=1}^{n_i} \lambda_i^j}{n_i N_u} = \frac{1}{n_i} \tag{9}$$

It is clear that $\text{MCS}_i \in (0, 1]$. In a decentralized control architecture, the effect of a sensor or communication related fault is confined to the cluster where it originates. Therefore, the MCS is an indicator of robustness to such faults - a small value indicates that the effect of failures is less widespread. Hence, it is desired to partition the system such that the corresponding MCS is small.

B. Stage-level combinatorial optimization

The objective of the stage level optimization (Fig. 1) is to appropriately split the parent clusters to obtain corresponding child clusters. This process is based on a combinatorial procedure explained below and illustrated in Fig. 2.

The parent clusters for stage S_i are the child clusters, $C_{i-1}^j, (j = 1, 2, ..., n_{i-1})$ from its preceding stage S_{i-1}. An *intermediate cluster pair* for any parent cluster is defined as a set of two non-empty and non-overlapping

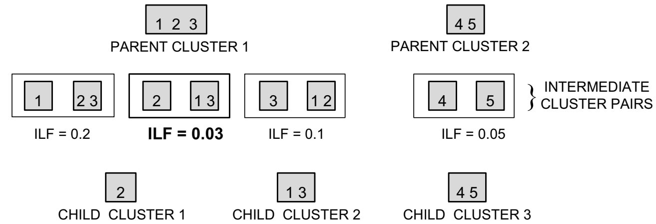

Fig. 2. Schematic of combinatorial optimization process for any given stage.

clusters obtained by splitting it. Therefore, the number of intermediate cluster pairs, $n_{i,j,int}$ obtained from the parent cluster C_{i-1}^j is given by the *Stirling number of the second kind* [20], $S(\lambda_{i-1}^j, 2)$:

$$n_{i,j,int} = S(\lambda_{i-1}^j, 2) = 2^{\lambda_{i-1}^j - 1} - 1 \tag{10}$$

The Intermediate Loss Factor (ILF) is then defined for each such intermediate cluster pair, $\{C_{i,j,int}^l, C_{i,j,int}^{*l}\}$ as :

$$\text{ILF}_{i,j,int}^l = \frac{\mathcal{C}\left(C_{i,j,int}^l, C_{i,j,int}^{*l}\right)}{\mathcal{C}\left(C_{i-1}^j, C_{i-1}^j\right)}, \tag{11}$$

$$\text{where,} \quad l = 1, 2, ...n_{i,j,int} \quad \text{and} \quad j = 1, 2, ...n_{i-1}.$$

The underlying optimization problem for the i^{th} stage S_i is to find the parent cluster (indicated by j^*) and its corresponding intermediate cluster pair (indicated by l^*) which yield the smallest ILF :

$$\{j^*, l^*\} = \underset{\{j,l\}}{\text{argmin}} \ \text{ILF}_{i,j,int}^l \tag{12}$$

The optimal parent cluster, $C_{i-1}^{j^*}$ is then split to create the optimal intermediate cluster pair, $\{C_{i,j^*,int}^{l^*}, C_{i,j^*,int}^{*l^*}\}$ whereas the other parent clusters are retained. The result is a set of child clusters having one more cluster than the set of parent clusters.

The $\text{ILF}_{i,j,int}^l$ defined in (11) measures the 'amount' of coupling ignored in the creation of the intermediate cluster pair $\{C_{i,j,int}^l, C_{i,j,int}^{*l}\}$ from the parent cluster C_{i-1}^j, normalized with respect to the coupling originally present in the parent. Therefore, the optimization (12) involves determination of the split with smallest resulting loss of coupling, among all possible splits.

C. MINCUT approximation

The exponential computational complexity characterized by (10), of the combinatorial optimization, motivates the development of a more tractable approach for the minimization problem (12). In what follows, for simplicity, we denote the size λ_{i-1}^j of the parent cluster C_{i-1}^j by n. The elements of C_{i-1}^j are accordingly denoted by p_r, where $r = 1, 2, ..., n$.

A matrix H_j is constructed for the j^{th} parent cluster, C_{i-1}^j, in a manner analogous to the construction of the coupling matrix in (5) :

$$H_j = \begin{pmatrix} H_{p_1,p_1} & H_{p_1,p_2} & \cdots & H_{p_1,p_n} \\ H_{p_2,p_1} & H_{p_2,p_2} & \cdots & H_{p_2,p_n} \\ . & . & \cdots & . \\ . & . & \cdots & . \\ H_{p_n,p_1} & H_{p_n,p_2} & \cdots & H_{p_n,p_n} \end{pmatrix} \tag{13}$$

For any given intermediate cluster pair, $\{C_{i,j,int}^l, C_{i,j,int}^{*l}\}$, a matrix, H_j^l can be obtained from H_j by setting to zero all blocks which correspond to elements in one intermediate cluster only. More precisely :

$$H_j^l = \begin{pmatrix} \theta_{p_1,p_1}H_{p_1,p_1} & \theta_{p_1,p_2}H_{p_1,p_2} & \cdots & \theta_{p_1,p_n}H_{p_1,p_n} \\ \theta_{p_2,p_1}H_{p_2,p_1} & \theta_{p_2,p_2}H_{p_2,p_2} & \cdots & \theta_{p_2,p_n}H_{p_2,p_n} \\ . & . & \cdots & . \\ . & . & \cdots & . \\ \theta_{p_n,p_1}H_{p_n,p_1} & \theta_{p_n,p_2}H_{p_n,p_2} & \cdots & \theta_{p_n,p_n}H_{p_n,p_n} \end{pmatrix} \tag{14}$$

Where,

$$\theta(p_r, p_s) = \begin{cases} 0 & \text{if } r, s \in C_{i,j,int}^l \text{ or } r, s \in C_{i,j,int}^{*l} \\ 1 & \text{otherwise} \end{cases} \tag{15}$$

Using the above definitions, $\mathrm{ILF}_{i,j,int}^l$ defined in (11) can be expressed as :

$$ILF_{i,j,int}^l = \frac{\left|\left|H_j^l\right|\right|_2}{\left|\left|H_j\right|\right|_2} \tag{16}$$

From the above expression, the problem of minimizing $\mathrm{ILF}_{i,j,int}^l$, over intermediate cluster pairs indexed by l, for a particular parent, denoted by a fixed j, corresponds to the minimization of $\left|\left|H_j^l\right|\right|_2$ over l. Assuming that H_j^l is sufficiently sparse, we now approximate $\left|\left|H_j^l\right|\right|_2$ by the 2-norm of the vector v_j^l consisting of the elements of H_j^l.

To make this more formal, we introduce a binary vector $x \in \mathbb{R}^n$ whose elements, x_r are defined as follows :

$$x_r = \begin{cases} 1 & \text{if } p_r \in C_{i,j,int}^l \\ -1 & \text{if } p_r \in C_{i,j,int}^{*l} \end{cases} \tag{17}$$

The square of the 2-norm of v_j^l can easily be stated as :

$$\left|\left|v_j^l\right|\right|_2^2 = \frac{z^T Q^T H_p^{.2} Q z - x^T Q^T H_p^{.2} Q x}{2} \tag{18}$$

Here, $H_p^{.2}$ denotes the matrix obtained by taking element-wise square of H_p. The quantities Q and z are defined below :

$$Q = \begin{pmatrix} e & 0 & \cdots & 0 \\ 0 & e & \cdots & 0 \\ . & . & \cdots & . \\ . & . & \cdots & . \\ 0 & 0 & \cdots & e \end{pmatrix}_{N.n \times n} \tag{19}$$

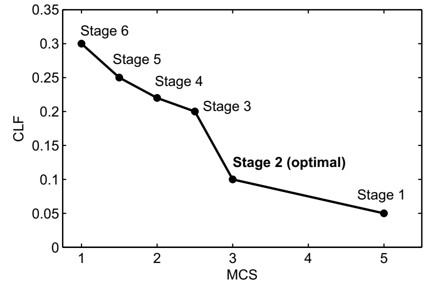

Fig. 3. Illustrative example of CLF vs. MCS plot.

$$z = [1\ 1\ \ldots\ 1]_{n \times 1}^T \tag{20}$$

Here, $e = [1\ 1\ \ldots\ 1]_{N \times 1}^T$

Hence, the problem of minimizing $\mathrm{ILF}_{i,j,int}^l$ over l for a particular parent j can be approximated by the following Boolean maximization :

$$\begin{aligned} \text{maximize} \quad & x^T Q^T H_p^{.2} Q x \\ \text{subject to} \quad & x_r \in \{1, -1\} \end{aligned} \tag{21}$$

The above maximization can be performed using numerical techniques such as [21] available for solving the MINCUT problem. In this way, for each parent j, the minimum ILF can be found and compared across all parents to solve the original minimization problem (12)

D. Optimal Stage Selection

Since it is desired to have both CLF and MCS small, this problem is analogous to dual objective optmization in a pareto-optimal setting [22]. Motivated by this, the optimal stage S_{i^*} is obtained from a plot of CLF_i versus MCS_i (Fig. 3).

The optimal stage should be a knee point. Therefore, navigating along the curve about that point in either direction would result in a large increase in one metric but only a relatively small decrease in the other metric. The plot must be studied in the ascending order of the partitioning stages (right to left) for knee points. For instance, if the first knee is not 'sufficiently' sharp, then the second knee should be studied.

IV. Case Study

An example is presented in this section to demonstrate the application of the proposed clustering procedure.

A. Test System Description

The layout of the building used in this example is shown in Fig. 4. It consists of 3 floors, with a total of 9 rooms of equal dimensions ($5 \times 5 \times 5\ m^3$) numbered as shown. The walls were modeled as RC circuits (Fig. 5) based on the accessibility factor method described in [16], and the zones were modeled as isolated capacitors. Each room has 6 walls - 4 side walls, 1 ceiling and 1 floor. The construction details are presented in Table I, from which the resistances and capacitance for each wall were computed. The zonal thermal capacities were assumed

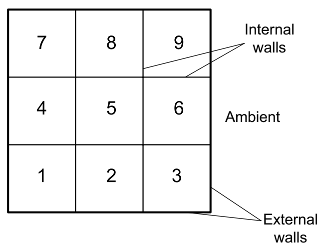

Fig. 4. Test building architecture (Side view).

TABLE I
Test Building Parameters [15]

Element	Layering	Thickness (m)
External walls	Brick	0.122
	Insulation	0.050
	C-Block	0.112
	Plaster	0.013
Internal walls	Plaster	0.013
	C-Block	0.122
	Plaster	0.013

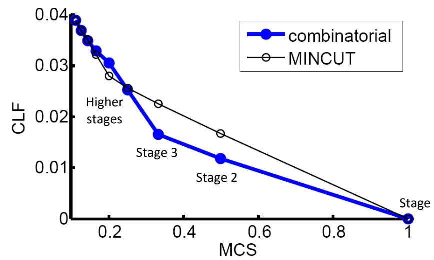

Fig. 6. CLF vs. MCS plot for $\rho = 1$

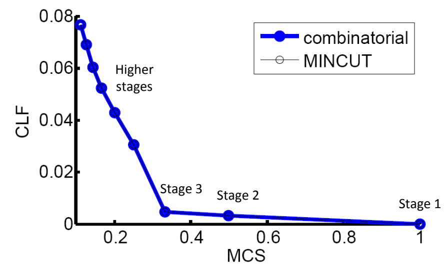

Fig. 7. CLF vs. MCS plot for $\rho = 2$

to be 250 kJ/K based on air at 25 C and 10^5 Pa. An overall system model of the form (1) was obtained by constructing an RC network using these details, followed by discretization using the zero-order-hold method with step size of 10 minutes (close to one-tenth of the smallest time constant in the model).The Hessian Matrix, H_k was then created with prediction horizon, $N = 24$ samples (4 hours).

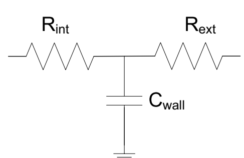

Fig. 5. Wall RC model depiction [16].

The inner and outer resistance values in Fig. 5 for all horizontal and vertical internal walls were found to be the same as expected due to symmetry. We denote this value by R_{nom}. In the case study presented, the resistances of the horizontal internal walls are altered by a factor of $\rho > 0$, i.e. $R_H = \rho R_{nom}$. Correspondingly, the resistances of the vertical internal walls are scaled by a factor of $1/\rho$, i.e. $R_V = R_{nom}/\rho$. Therefore, the ratio R_H/R_V is amplified by ρ^2. The clustering methodology presented in Section III was applied for various values of the factor ρ.

B. Results

The CLF vs. MCS plots for some selected values of ρ are shown in Fig. 6 to 8 . Key observations are as follows :

1) The CLF vs. MCS plots using the MINCUT procedure and the combinatorial procedure exactly coincide in Fig. 7 and 8. However, they differ in Fig. 6. This suggests that the MINCUT approximation to the combinatorial optimization problem can be potentially accurate in asymmetric situations. In general, it trades accuracy for computational simplicity as indicated by a run-time of 0.29 seconds when compared to 4.92 seconds for the combinatorial procedure [3].
2) For the nominal case ($\rho = 1$), a knee point is not immediately obvious in Fig. 6. Therefore, stage 3 was chosen to be the optimal clustering where both CLF and MCS are satisfactorily small.
3) When $\rho > 1$, the optimal cluster set (child clusters pertaining to stage 3 in Fig. 7 and 8) obtained is :$\{\{1, 2, 3\}, \{4, 5, 6\}, \{7, 8, 9\}\}$. When $\rho < 1$, (resulting CLF vs. MCS plots not shown) the corresponding optimal cluster set is : $\{\{1, 4, 7\}, \{2, 5, 8\}, \{3, 6, 9\}\}$. This can be justified on the basis of physical arguments. When $\rho > 1$, the horizontal walls are more insulating than the vertical walls, therefore the clusters must be sliced horizontally. A similar explanation applies to the case $\rho < 1$.

C. Discussion

The results of the clustering procedure were easily explained on the basis of physical intuition for the chosen case study. This encourages its implementation on more complex cases in the future. Additionally, the approach can work with existing system information, e.g. Building Information Management (BIM) systems, to get physical information that can drive accurate analyses. The computational complexity of the combinatorial optimization algorithm is an important concern. The processing

3. Values are for the case $\rho = 1$, implemented on a 2.0 GHz, 960 MB, AMD Athlon machine

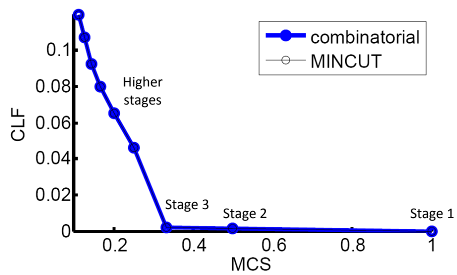

Fig. 8. CLF vs. MCS plot for $\rho = 3$

time would scale with the complexity of the system. To address this problem, computationally tractable methodologies which are more reliable than the presented MINCUT approximation are required. This aspect is an open question currently under study.

V. Conclusions

A combinatorial optimization based clustering procedure, together with its MINCUT approximation was presented in this paper for the determination of appropriate decentralized control architectures in the context of building thermal control. Optimality and robustness were quantified in the form of CLF and MCS metrics, respectively, and the partitoning process involved achieving a tradeoff between these two objectives. Application of this appoach on a medium-scale building system resulted in physically justifiable choices of control clusters. Decentralized control design based on the clusters obtained by the method proposed in this paper will be undertaken in future.

References

[1] EIA, "Annual energy outlook 2009," 2009. [Online]. Available : http ://www.eia.doe.gov/oiaf/aeo/emission.html

[2] G. Huang, S. Wang, and X. Xu, "A robust model predictive control strategy for improving the control performance of air-conditioning systems," *Energy Conversion and Management*, vol. 50, no. 10, pp. 2650–2658, 2009.

[3] D. Kolokotsa, A. Pouliezos, G. Stavrakakis, and C. Lazos, "Predictive control techniques for energy and indoor environmental quality management in buildings," *Building and Environment*, vol. 44, no. 9, pp. 1850–1863, 2009.

[4] S. Bushby and H. Newman, "BACnet today," *ASHRAE Journal*, vol. 10, pp. 10–18, 2002.

[5] S. Wang and Z. Ma, "Supervisory and optimal control of building HVAC systems : A review," *HVAC&R Research*, vol. 14, no. 1, pp. 3–32, Jan 2008.

[6] E. Mathews, C. Botha, D. Arndt, and A. Malan, "HVAC control strategies to enhance comfort and minimise energy usage," *Energy and Buildings*, vol. 33, no. 8, pp. 853–863, 2001.

[7] P. Campo and M. Morari, "Achievable closed-loop properties of systems under decentralized control : Conditions involving the steady-state gain," *Automatic Control, IEEE Transactions on*, vol. 39, no. 5, pp. 932–943, 1994.

[8] P. Davidsson and M. Boman, "Distributed monitoring and control of office buildings by embedded agents," *Information Sciences*, vol. 171, no. 4, pp. 293–307, 2005.

[9] S. Sharples, V. Callaghan, and G. Clarke, "A multi-agent architecture for intelligent building sensing and control," *Sensor Review*, vol. 19, no. 2, pp. 135–140, 1999.

[10] B. Huberman and S. Clearwater, "A multi-agent system for controlling building environments," in *Proceedings of the First International Conference on Multi-Agent Systems (ICMAS-95)*, 1995, pp. 171–176.

[11] J. Sandhu *et al.*, "Wireless sensor networks for commercial lighting control : decision making with multi-agent systems," in *AAAI workshop on sensor networks*, 2004, pp. 131–140.

[12] W. Kastner, G. Neugschwandtner, S. Soucek, and H. Newmann, "Communication systems for building automation and control," *Proceedings of the IEEE*, vol. 93, no. 6, pp. 1178–1203, 2005.

[13] V. Chandan, S. Mishra, and A. Alleyne, "Predictive control of complex hydronic systems," in *American Control Conference (ACC), 2010.* IEEE, 2010, pp. 5112–5117.

[14] G. Henze, D. Kalz, C. Felsmann, and G. Knabe, "Impact of forecasting accuracy on predictive optimal control of active and passive building thermal storage inventory," *HVAC & R Research*, vol. 10, no. 2, pp. 153–178, 2004.

[15] M. Gouda, S. Danaher, and C. Underwood, "Building thermal model reduction using nonlinear constrained optimization," *Building and Environment*, vol. 37, no. 12, pp. 1255–1265, 2002.

[16] F. Lorenz and G. Masy, "Méthode d'évaluation de l'économie d'énergie apportée par l'intermittence de chauffage dans les bâtiments," *Traitement par differences finies d'un model a deux constantes de temps, Report No. GM820130-01. Faculte des Sciences Appliquees, University de Liege, Liege, Belgium*, 1982.

[17] G. Hudson and C. Underwood, "A simple building modelling procedure for MATLAB/SIMULINK," in *Proceedings, International Building Performance and Simulation Conference, Kyoto*, 1999.

[18] V. Chandan, "Modeling and control of hydronic building hvac systems," 2010. [Online]. Available : http ://www.ideals.illinois.edu/bitstream/handle/2142/16204/chandan_vikas.pdf ?sequence=1

[19] S. Skogestad and I. Postlethwaite, *Multivariable feedback control : analysis and design.* Wiley New York, 1996.

[20] G. Rota, "The number of partitions of a set," *American Mathematical Monthly*, pp. 498–504, 1964.

[21] M. Stoer and F. Wagner, "A simple min-cut algorithm," *Journal of the ACM (JACM)*, vol. 44, no. 4, pp. 585–591, 1997.

[22] S. Boyd and L. Vandenberghe, *Convex optimization.* Cambridge Univ Pr, 2004.